Protection of Warm elements at IR7, passive absorbers and collimators

Magistris M., Santana Leitner M, Vlachoudis V., Ferrari A.

November 15, 2006

Abstract

This report revises the annual dose deposition in objects that, although not needing to vouch for a superconducting regime, nor containing delicate electronic circuits, still cannot stand arbitrarily high levels of radiation. Among them there is the epoxy used in the insulator blocks or in the coils of the magnets, the pipes whose wrapping film must ensure the heating during out-gassing, the flanges, where asymmetric irradiations can cause pressure in-leaks, or the collimators, whose jaws must remain flat to function properly. The addition of passive absorbers and the use of appropriate materials shall guarantee a correct operation of all these objects.

Contents

1 Introduction

1.1 Simulations of the IR7 insertion

The collimation system of the future Large Hadron Collider (LHC) at CERN is a challenging project since the transverse intensities of the LHC beams are three orders of magnitude greater than those of other current facilities. Two insertions (IR3, IR7) of LHC are dedicated to beam cleaning with the design goal of absorbing part of the primary beam halo and of the secondary radiation. These insertions will house 54 movable two-sided collimators, and will be among the most radioactive areas of LHC. The collimators should withstand the deposited power, which for phase I can reach values of about 25 kW in the upstream units ($\sim$3 kW in the jaws).

The tertiary halo that escapes the collimation system in IR7 could heat some fragile elements up to unacceptable levels, if no additional absorber were used. In order to assess the energy deposition in sensitive components, extensive simulations were run with the Monte Carlo cascade code FLUKA[1, 2].

1.2 Sensitive warm components

This report revises the annual dose deposition in objects that, although not needing to vouch for a superconducting regime, nor containing delicate electronic circuits, still cannot stand arbitrarily high levels of radiation. Among them there is the epoxy used in the insulator blocks or in the coils of the magnets, the pipes whose wrapping film must ensure the heating during out-gassing, the flanges, where asymmetric irradiations can cause pressure in-leaks, or the collimators, whose jaws must remain flat to function properly. The addition of passive absorbers and the use of appropriate materials shall guarantee a correct operation of all these objects.

1.3 Passive absorbers for warm elements

Passive absorbers are shielding devices that are mounted around the vacuum pipe. Their aperture may be smaller than the upstream and downstream pipes in order to intercept a larger fraction of particles[1]. The *passive absorber* is generically named **PA**, and, more specifically, **TCLPA**[2] in contrast with **TCLA**[3, 4, 5], which stands for *active absorber*[3]. Simulations should provide a solution for the shape and position of the TCLPA in terms of the annual dose in the coils of the MBWB6L,

[1]However, this option is only possible if it meets the requirements of vacuum and beam dynamics.
[2]Depending on their position and length, names like **TCLSA** and **TCLQA** are also used.
[3]The TCLA invade the pipe with two jaws (half-gap: 10 σ and require active cooling).

MBWA6L and MQW[4]magnets 198 and First module of D3 and Q5, placed at about . These doses should stay below the threshold of 3 MGy/y to preserve the thin epoxy insulation around the cables and thus prevent disruptions[6]. Other sensitive components are the wrapping heaters in the pipes and the epoxy blocks stand between the upper and lower coils. Moreover, depending on the heat load in the TCLPA's themselves, water cooling may be required.

After some basic tests, the outer shape of the absorber was frozen at 45 x 45 cm in the x-y plane and to 100 cm in the longitudinal dimension (z). The inner longitudinal hole should match the aperture of the shielded element in order to maximize the efficiency to filter the off-axis particles and it should be located as close as possible to the protected element. However, space constraints (for smooth maintenance and mounting) impose minimal absorber-magnet distances. In the quest of an optimum configuration, several variables were looked at independently. The study started by the determination of the most harmful case between the vertical (*vert*) and the horizontal (*hori*) beam loss scenarios (sec. 2.1.1). Then, the annual dose was lowered by adjusting the length of the absorber (1 or 2 m), its position (at 50 or 10 cm from the MBWB), the inner opening dimensions (from arbitrary diameters to the aperture of the beam) and its material.

1.4 Normalization Factors

One of the goals of this work was to minimize the peak doses in the sensitive elements of the MBW and MQW magnets for every year (y) of irradiation. The normalization factor (counts $\left[\frac{GeV}{cm^3\ prot.}\right]$ $\rightarrow$ annual dose $\left[\frac{MGy}{y}\right]$) was obtained as:

$$F_n = \Phi\ \left[\frac{prot.}{y}\right] \cdot \rho^{-1}\ \left[\frac{cm^3}{kg}\right] \cdot 1.6 \cdot 10^{-13}\ \left[\frac{MJ}{GeV}\right] \tag{1}$$

where:

- The flux of losses Φ per beam are [7]:

$$Flux\left[\frac{p}{y}\right] = \begin{cases} 2.00 \cdot 10^{16} & \text{for ultimate luminosity}^5 \\ 1.15 \cdot 10^{16} & \text{for nominal luminosity} \end{cases} \tag{2}$$

- And the density:

$$\rho\left[\frac{g}{cm^3}\right] = \begin{cases} 1.43 & \text{in the insulators} \\ 7.18 & \text{in the coils} \end{cases} \tag{3}$$

[4]Warm dipole and quadrupoles placed about 172, 166 and 142 m upstream the IP7 interaction point.

The coils were simulated as plain copper objects, so that the density that was used to obtain the annual dose in the 'virtual' epoxy insulators was that of copper[6]. Moreover, unless otherwise stated, calculations have been performed for **ultimate luminosity**. Therefore:

1. The conversion factor was:

$$F_n\left[\frac{MGy\ cm^3\ p}{GeV\ y}\right] = \begin{cases} 444 & \text{for the epoxy of the coils}^7 \\ 2230 & \text{for the insulator blocks} \end{cases} \quad (4)$$

2. If applied to nominal operation, the above figures include a 40 % security margin.

The second goal is to compute the peak power densities and total powers in the magnets and in the absorbers. All power density $\left[\frac{GeV}{cm^3\ p}\right]$ and total power $[W]$ numbers in this report have been obtained by scaling the FLUKA results $\left[\frac{W}{cm^3}\right]$ by the factor $Fn = 57.6$, which corresponds to a loss rate of about $3.6 \cdot 10^{11}$ $\left[\frac{p}{s}\right]$, valid for the 0.1 h beam lifetime assumption at ultimate intensity [7][8].

2 Reduction of the annual dose in the MBWB6R and MBWA6R

The radiation progressively harms the insulators and, at some point, the damages may induce disruptions between conductors. This section first presents the sequential approach to shield the insulators in the coils of the MBW magnets so that their lifetime is maximized. The obtained configuration is then tested again loss scenarios other than the design one (horizontal losses, nominal conditions). As for the heating film around the pipes, also rather delicate against radiation, it is surveyed separately in section 5.1.

2.1 Dose minimization scheme for the MBW insulators at horizontal losses

Results for all the following configurations are summarized in Table 1

2.1.1 No passive absorber (PAabs)

The initial step was to check whether any absorber was required at all to shield the sensitive components in the warm MB's. Simulations were launched with

[6] In fact, the density of 7.18 $\frac{g}{cm^3}$ is lower than that of Cu (8.92 $\frac{g}{cm^3}$) because it includes the water cooling circuits within the coils.

[8] This number may have been refined since the completion of our computations.

the settings and scorings described in appendix A for the horizontal beam loss scenario and the results were scaled with the F_n value discussed in 1.3 ($F_n = 444\left[\frac{MGy\ cm^3\ p}{GeV\ y}\right]$). These were the conclusions of the simulations:

- † The peak annual dose in the coils of the MBWB6R without absorber (PAabsent) reaches **85 MGy/y**, (28 times the recommended peak dose) at the inner surface of the upper coil in the front crossing over the beam.
- † The peak annual dose in the symmetric coil (lower coil) is 75 MGy/y.
- † The annual dose in the rear part of the MBWB and in the MBWA is lower ($\sim$ 50 and 25 MGy/y, respectively).

2.1.2 A tight Steel absorber (PAFe)

The second step consisted in placing a block of steel as described in app. A.2, with a hole that would match exactly the pipe, that is, an ellipse of semi $\hat{x}$-axis 2.95 cm and $\hat{y}$ 2.2 cm. This ought to filter a great number of the halo particles. Otherwise, following the same methodology as in sec 2.1.1, it was found that:

- † The peak doses in MBWB drops to about 4.8 and in MBWA to 3.9 MGy/y, thus a factor 20 reduction was achieved for MBWB, but the doses in MBWB and MBWA were still too high.
- † Further optimization was therefore required. However, there was no certainty passive absorber could at all manage to lower the doses below admisible values[9]. This extreme possibility was checked by simulating an ideally absorbing block of the same dimensions (sec.2.1.3).

2.1.3 A tight ideal absorber (PAbckh)

The third step addressed the questionmark raised in sec.2.1.2 about the maximum shielding capacity of the passive absorbers. For that sake, the absorber material was taken as an ideal black(body)box that acts as a perfect sink for all impinging particles. The results were the following:

- † The annual dose would then not exceed 0.5 MGy/y for the MBWB and 1.5 MGy/y for the MBWA.
- † This ideal limit could be approached by having a longer (eg. two meter) absorber or/and high Z material (eg. W).

[9]That is, not reducing the aperture of the machine.

At this point, it became clear that the length of the absorber was constrained to about 1 meter due to the dense packing of equipment in the area. Therefore, the sole direction of improvement came from the choice of material, tungsten (sec.2.1.4).

2.1.4 A tight good absorber; tungsten block (PAW)

The fourth step was then a mere material transformation from black-hole to its closest absorbing real (affordable) material: tungsten. These were the conclusions:

† With a 1m-W absorber, the doses don't exceed 2 MGy/y and 1.9 MGy/y in the front and rear coils of MBWB, and 3.9, 2.5 MGy/y for MBWA.

† These values are close to be acceptable, although they could be improved in MBWA by inserting a thin absorber between MBWB and MBWA.

† Looking at the doses in the MBWA, and specially comparing the case of no absorber (section 2.1.1) with the rest, it is remarked that the annual dose in the second magnet is roughly independent of the presence of the passive absorber, and, thus, that the first magnet is acting as an absorber itself. Therefore, it could be interesting to place a real absorber just before MBWA (see the following section, 2.1.5).

2.1.5 A tight good absorber + a thin intermediate mask (PAWsW)

The last step in the process of shielding the MBW pair consisted in the insertion of a 20 cm tungsten absorber (TCLS) between the two MBW (still keeping the tungsten absorber just defined on page 8) to minimize the annual dose in the second MBW. The *prototype.pos* file then looked like:

```
...
# Passive Absorbers (1 m long)
TCLP   1 1 PA_BODY    -2000.0   0.0   -750.0    100.0 -
# Passive Absorbers (0.2 m long)
TCLS   1 1 PAsBODY    -2000.0   0.0   -680.0     20.0 -
...
```

This action was quite positive and lowered the peak doses to acceptable levels. These were the conclusions:

† The effect of adding an intermediate 20 cm-W absorber does not rise the annual dose in the MBWB (negligible backscattering).

† The peak annual dose in the front crossing of the coils in MBWB with the 1 m-W absorber + 20 cm-W absorber is 1.9 MGy/y, while this value remains around 1.8 MGy/y for the back crossing ($\pm 4\%$)

† The peak annual dose in the front crossing of the coils in MBWA with the 1 m-W absorber + 20 cm-W absorber is 1.8 MGy/y, while this value remains around 2.4 MGy/y for the back crossing ($\pm 4\%$)

Case	Absorber	F_MBWB	B_MBWB	Absorber	F_MBWA	B_MBWA
2.1.1	$\emptyset$	85	>50	$\emptyset$	25	-
2.1.2	100 cm-Fe	4.8	-	$\emptyset$	3.9	-
2.1.3	100 BH	0.5	-	$\emptyset$	1.4	-
2.1.4	100 cm-W	2	1.9	$\emptyset$	3.9	2.5
2.1.5	100 cm-W	2.0	1.8	20 cm-W	1.8	2.4

Table 1: Dose peaks (maximum between upper and lower coil) $[\frac{MGy}{y}]$ in the front (F) and back (B) coils of MBWB and MBWA for different shielding configurations at the horizontal loss scenario, top energy, ultimate luminosity. (-) Means that the value has not been recorded.

2.2 Validation of the MBW-shielding solution in different scenarios

The probe scenario has been that of *horizontal* losses at *top* beam energy (*hori-lwb*). Obviously, the study would be incomplete without the computation of the equivalent *vert-lwb* case[10].

Table 2 gathers the peak doses in the MBW coils for both the vertical and the horizontal loss scenarios at top energy and ultimate luminosity.

Case	*TCLPA*	F_MBWB	B_MBWB	*TCLSA*	F_MBWA	B_MBWA
hori *2.1.5*	*81*	2.0	1.8	*18*	1.8	2.4
vert	*83*	1.5	1.6	*22*	1.9	1.9

Table 2: Dose peaks (maximum between upper and lower coil) $[\frac{MGy}{y}]$ in the front (F) and back (B) coils of MBWB and MBWA and *power density* $[\frac{W}{cm^3}]$ *in the first two passive absorbers* for the vertical and horizontal loss scenarios at top energy, nominal conditions (Gy: $2 \cdot 10^{16}$ lost protons/y) and 0.2h loss scenario (W: $4 \cdot 10^{11}$ lost protons/s).

From the numbers in *table 2* it can be concluded that:

† The horizontal beam loss scenario is about 20 % more severe in the MBW than the vertical loss scenario.

† The loss patterns for the vertical and horizontal loss scenarios are equivalent in the dogleg bending magnets.

[10] Ideally the *skew-lwb* condition should be analyzed too.

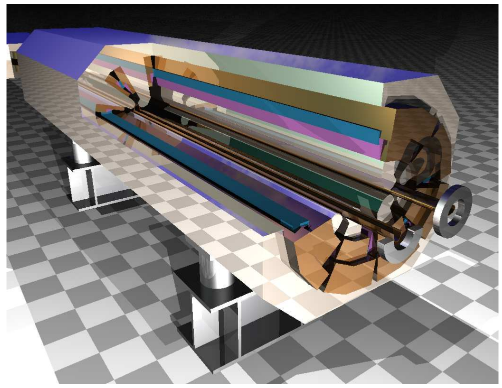

Figure 1: Open PovRay view into an MQW magnet as implemented in IR7 with FLUKA

As for the *injection* loss scenarios (*vert/hori-inj*), they are not so important for the yearly doses since they don't happen during long enough periods to integrate noticiable damages in the insulators. Nonetheless, the power deposited in the passive absorbers may be an issue. This case is studied in section 6.

Another set of commissioning failure scenarios is that where the secondary collimators remain retracted *acc-(vert/hori)-(inj/lwb)*. Again, this shall not give way to worrysome doses because the malfunction, if any, would be temporary, and also because the first secondary collimator is downstream of MBWA[11].

3 Reduction of the annual dose in MQWAEA5 and MQWADA5

The procedure initiated in 2.1 for the test case of horizontal beam losses is here resumed to shield the coils of the MQWA magnets. Then, like for the MBW, the final solution is confronted to other loss scenarios. Again, other sensitive components of the MQW's are separately treated in section 5.

3.1 Dose rate minimization of the MQWA coils

3.1.1 No extra absorber for MQW (PAWsW)

The initial step was to check whether any extra absorber was required at all to shield the sensitive components in the warm MQ's. Simulations were launched with the settings and beam (horizontal losses) described in section 2.1.5 with annual dose scorings along the MQWAE and MQWAF. The results (directly obtained

[11] However, this case is relevant for the passive absorber that shields the MQW, placed just downstream the first TCSGA6L1.

by FLUKA in Gy/p) were scaled, as for section 2, by $F_n = 2 \cdot 10^{16} \frac{p}{y}$ to have MGy/y for the ultimate luminosity.

† The annual dose distribution in the MWQA's is symmetric with respect to the xz plane.

† The peak annual dose in the coils of the MQWAE5R with a thick W (1 m) absorber before MBWB and a thin one (0.2 m) in between MBWB and MBWA (PAlimWsW) reaches **13 MGy/y** $\pm$ **16%**, (8 times the recommended peak dose) in the closest horizontal coil (x = 18.5, y = $\pm$ 0.5) at a depth of 22 cm from the front plane of the MQW.

† The peak annual dose in the iron of MQWAE reaches **200 MGy/y** $\pm$ **1%** at 13.5$\pm$1.5, depth = 13 cm

† The peak annual dose in the coils of the MQWAD, placed after MQWAE with the same shielding conditions, is lower than in MQWAE, the value being **4 MGy/y** $\pm$ **4%** in the closest horizontal coil (x = 18.5, y = $\pm$ 0.5) at the front face of the magnet.

3.1.2 An additional short absorber before MQWAE (PAWsWsW)

In the second step a thin block[12] of tungsten (lack of space justifies the choice of W instead of Steel) was inserted as shielding, with a hole that would match exactly the pipe, that is, an ellipse of semi axis $\hat{x}$-axis 2.55 cm and $\hat{y}$ 1.45 cm. This should filter a great fraction of the halo. The file *prototype.pos* now looks like that:

```
...
# Passive Absorbers (1 m long)
TCLP   1 1 PA_BODY     -2000.0   0.0   -750.0     100.0 -
# Passive Absorbers (0.2 m long)
TCLS   1 1 PAsBODY     -2000.0   0.0   -680.0      20.0 -
TCLQ   1 1 PAsMQW      -2000.0   0.0   -650.0      20.0 -
...
```

A close examination of the results with the extra TCLQ absorber casts the following conclusions:

† The total heat deposited in MQWAE drops from 32.7 to 16.0 kW, and from 8.3 to 5.8 kW in MBWAD. The next four MQ's (AC,B,AB,AA) get 4.4, 3.3, 3.1 and 2.7 kW instead of the 5.9, 4.3, 3.9 and 3.3 kW that they would receive without the shielding.

† The absorber TCLQ itself absorbs a total of power of 25 kW.

[12] 45 x 45 x 20 cm^3.

- † The peak annual dose in the coils of the MQWAE5L goes down to ∼4 MGy/y, three times less than the bare case. As for MQWAD5L, the peak dose is reduced by a factor 2.
- † Fig 3(a) shows that the peak is very close to the boundary of the coil, so its value may be slightly overestimated by the mixing-up of different densities in a same scoring bin.

3.1.3 An extended absorber before MQWAE (PAWsWmW)

The peak doses in MQWAEL5 still being fairly high, it was decided to study the goodness of a longer (20 cm → 60 cm) absorber, TCLQ. The return of the coils was coarsely implemented for this iteration in order to discard higher annual dose peaks in that area, which had not yet been inspected:

	Magnet →	MQWAE		MQWAD	
Case ↓	Absorber	Peak	Total	Peak	Total
3.1.1	∅	13	16.3	4	4.2
3.1.2	20 cm-W	4	8	2	5.9
3.1.3	60 cm-W	$\lesssim$2.6	10.8	$\lesssim$ 2.3	6.3

Table 3: Dose peaks $[\frac{MGy}{y}]$ in the coils of MQWAE.L7.B1 and MQWAD.L7.B1 and integrated power (full magnet) $[kW]$ for different shielding configurations.

Fig.3.1.3 displays the annual dose maps in several zones of the MQWAE magnet with the protection of the 60-cm long W block.

- † The total heat deposited in MQWAE drops down to 10.8 kW, and to 6.3 kW in MBWAD. The next four MQ's (AC,B,AB,AA) get 4.4, 3.1, 3.0 and 2.6 kW, that is, about 5 % less than with the 20 cm long absorber.
- † The absorber TCLQ (60 cm long) absorbs a total of power of 35 kW, 10 kW more than the case with the short absorber (20 cm long) introduced in section 3.1.2.
- † The peak annual dose in the coils of the MQWAE5L goes below ∼2.6 MGy/y, five times less than the bare case. As for MQWAD5L, the peak dose is reduced to 2.3 MGy/y.

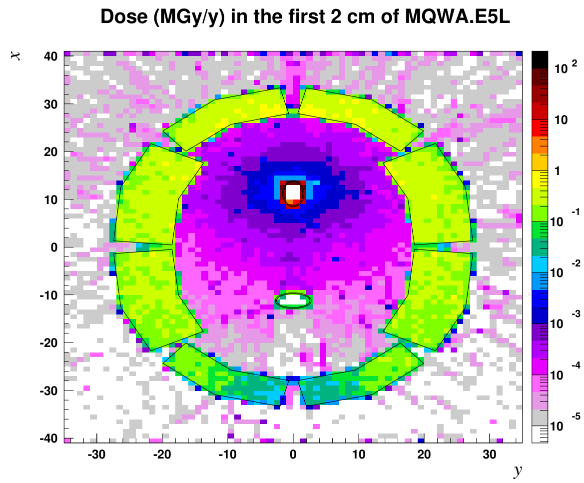

(a) MQWAE5L without dedicated absorber

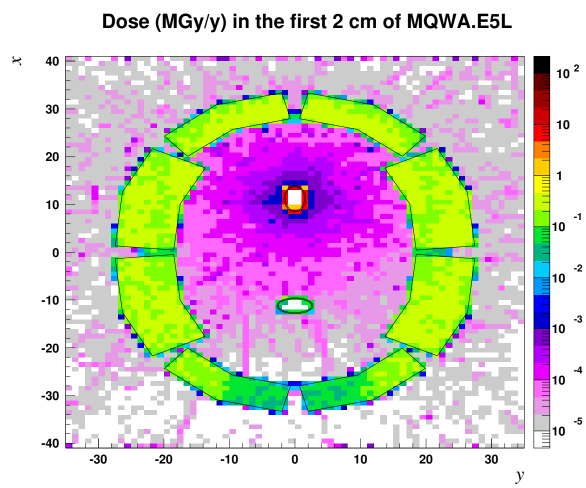

(b) MQWAE5L with a 20 cm long W absorber

Figure 2: Dose (MGy/y) maps in MQWAE5L with a 20 cm long W absorber

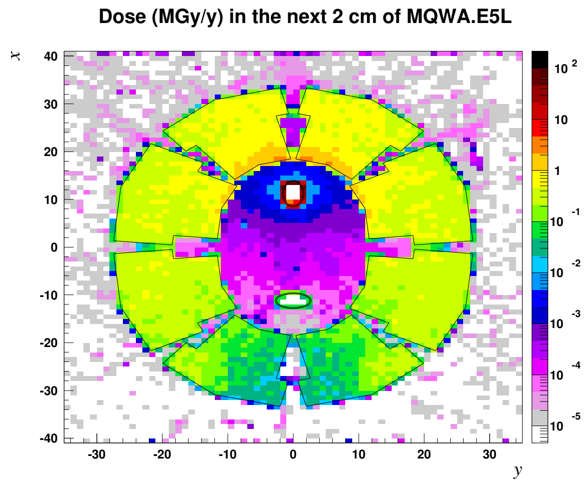

(a) MQWAD5L without dedicated absorber

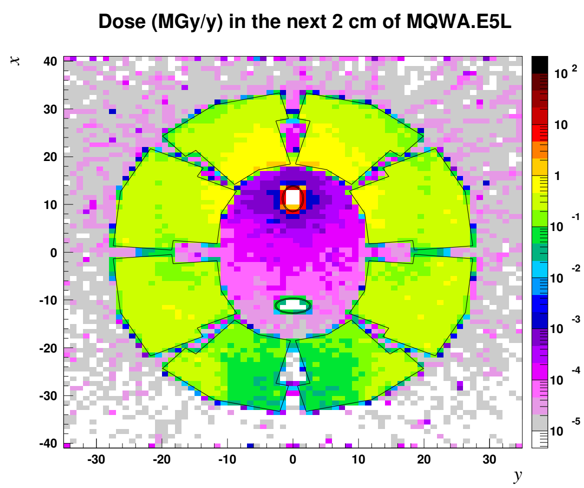

(b) MQWAD5L with a 20 cm long W absorber

Figure 3: Dose (MGy/y) maps in MQWAD5L

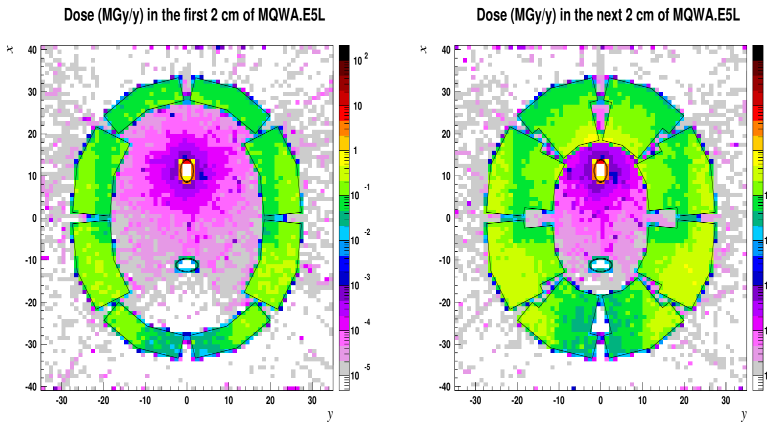

(a) First 2 cm (coil return)

(b) Next 2 cm (coil return)

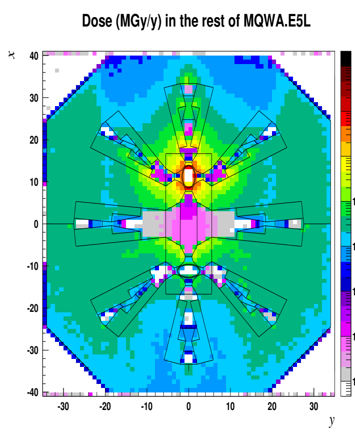

(c) Next 2 cm

Figure 4: Cross sectional annual dose (MGy/y) maps in MQWAD5L behind a 60-cm long W block matching the inner pipe size.

3.2 Validation of the MQW-shielding solution in different scenarios

To conclude this subject, a simulation with the vertical beam losses was carried out with the same configuration of passive absorbers. Results displayed in *table* 3.2 indicate that:

- † To what concerns the annual dose deposition in the MQW magnets, the horizontal and the vertical beam loss scenarios are equivalent.
- † Between the first two MQW's, the highest annual dose for both scenarios is registered in the second one, MQWAD.L7.B1, but the dose in the downstream objects is expected to damp down, as indicated by the total heat deposition (10.8, 6.3, 5.1, 4.0, 3.8 and 3.4 kW from MQWAE5L to MQWAA5L, horizontal case, ans similarly for the vertical scenario). The first and second MQW's act as absorbers themselves.

	Magnet →	MQWAE		MQWAD	
Case ↓	Scenario	Peak	Total	Peak	Total
3.1.3	Horizontal	$\lesssim$ 2.6	10.8	$\simeq$ 2.8	6.3
3.2	Vertical	$\lesssim$ 2.3	10.0	$\lesssim$ 2.8	5.7

Table 4: Dose peaks $[\frac{MGy}{y}]$ in the coils of MQWAE.L7.B1 and MBWAD.L7.B1 and integrated power (full magnet) $[kW]$ for the **hori**zontal and **vert**ical beam loss scenarios, with the shielding configurations defined in 3.1.3 for ultimate beam loss, $2 \cdot 10^{16}$ $[\frac{p}{y}]$.

4 Remarks and Conclusions about passive absorbers

The 200-mm long passive absorber in between the D3 modules couldn't actually fit in the IR7 layout as is. Indeed, the 2 x 200 and 300 extra mm that need to be accounted for the (2) quick connection vacuum flanges and for the additional bellow, respectively, demand more space than available. Thus, it has been suggested [8] to increase the inter-module space from 300 to 1000 mm by shifting each module in opposite directions and equal distances. This leaves the magnetic center unchanged.

Name	Z	Length	Heat	MBWB		MBWA		MQWAE	
	[m]	[m]	[kW]	Bare	Shiel.	Bare	Shiel.	Bare	Shiel.
TCLPA.1L7	22.77	1.0	27.5	85	2	25	3.8	>13	>13
TCLPA.2L7	23.87	0.2	2.60	2	2	3.8	2.4	>13	13
TCLPA.3L7	55.78	0.6	34.6	2	2	2.4	2.4	13	1.8

Table 5: Passive Absorber names/locations (from IP7), peak heat load, and impact on reduction of the peak doses [$\frac{MGy}{y}$] in the protected magnets.

5 Dose rate in the pipes and flanges

5.1 Dose rate in the wrapping of the MBW pipes

The pipes are typically outgassed by a heating system that forms a wrapping foil of some 300 μm thickness. This element is fragile to high radiation doses.

In the present case we are just interested to know the annual dose in the pipe, very thin when compared to other objects, so it would be convenient to set a very fine mesh to have trustful dose deposition results. In order to achieve that, the detection volume should match the pipe shape so that there is no excessive memory consumption in areas of no interest. However, this is not possible because FLUKA can score events in cartesian and cylindric (excentric-free) meshes but not in elliptical zones (like the MBW and MQW pipes).

Thus, a compromise cartesian grid of bin size 1 x 1 x 5 mm^3 was chosen. Results that appear in fig. 5(a) should be interpreted having in mind the previous asset. These were the conclusions for the horizontal beam loss case:

† The peak annual dose in the periphery of the pipe reaches the range 10-25 MGy/y

† The highest annual dose is in the horizontal plane. A heating along the vertical axis would only suffer from 4-12 MGy/y

† The ratio dose$_{\{horizontal\}}$ / dose$_{\{vertical\}}$ is around 3-8

5.2 Dose rate in the wrapping of the MQW pipes

The pipe inside MQW is, like that in MBW, elliptical, so we have the same memory consumption/precision conflict as with MBW (sec.5.1). Therefore, results shown in fig. 5(b) should be again cautiously interpreted.

† The peak annual dose in the periphery of the pipe is below 20 MGy/y.

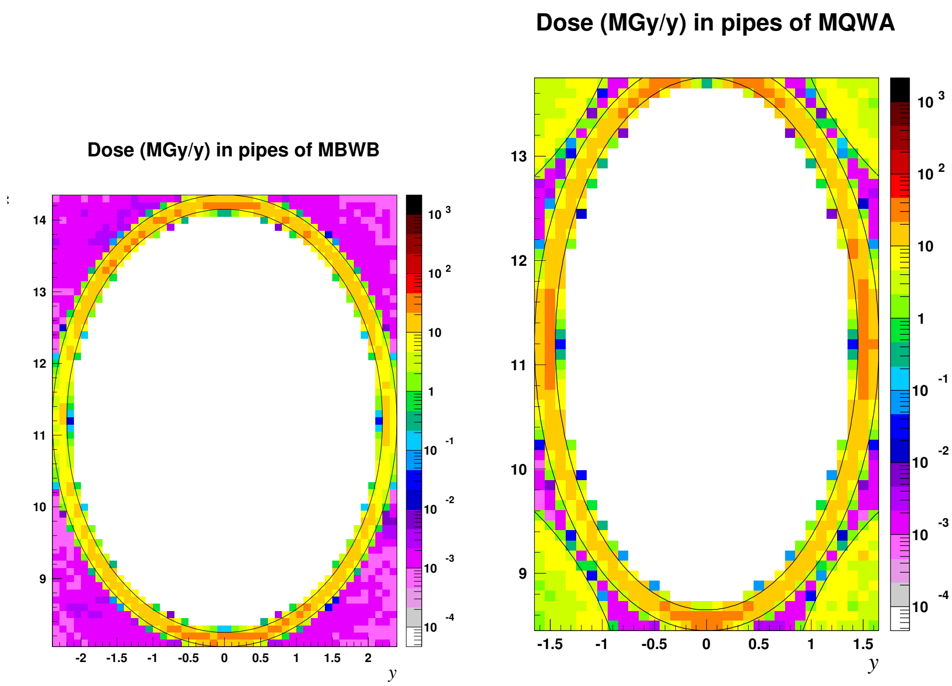

(a) MQWAE5L without dedicated absorber

(b) MQWAE5L with a 20 cm long W absorber

Figure 5: Dose (MGy/y) maps in the (a)MBWB and (b)MQWAE pipes for 0.1h beamlife time horizontal loss scenario losses at top energy and ultimate intensity.

† The annual dose is more moderate than in MBWB (fig. 5(a)).

† The external annual dose in the zones at 45 degres is lower than in the main axis, typically in the range 4-10 MGy/y.

6 Energy deposition peaks in the passive absorbers

The absorbers designed in sections 2 to 3 intercept a fairly intense and energetic flux of particles that leave behind large amounts of power. Thus, cooling issues might arise, which make it advisable to estimate the total and peak power depositions in the three passive absorbers. This situation is analyzed for standard operation, for injection and for an anomalous typified case where the collimators[13] are retracted.

6.1 Methodology

As introduced in section A.3 the card **usrbin_36** contains a 1 x 1 x 2 cm^3 $\{x, y, z\}$ mesh grid scoring per passive absorber.

Simulations were run with the settings for the *warm* section and for all possible combinations: $\{lwb, inj\} \otimes \{hori, vert\} \otimes \{nom, acc\}$[14]. Cross sectional plots were obtained by using a customized version of *plotxyxz.sh* ($ plotTCL.sh 36 3). Peaks where parsed by means of *getstat* (chapter B.1.3), applied to the formatted file that collects results of usrbin_36, usrbinf_36, with *None* mask and with a scaling factor of *57.6*[15], to obtain $\frac{W}{cm^3}$.

6.2 Results and conclusions

These were the conclusions of the simulations, the results of which are summarized in table 6:

† The beam spot is broader at injection, but the energy is 15 times lower than at top energy. The calculations indeed show that the power deposition at injection is well below that at top energy, specially for the second and third passive absorbers.

† Whatever the case, the most irradiated absorber is the third.

[13] in particular TCSGA6L1, sitting in front of TCLPQ.

[14] "acc" is a commissioning case where the jaws of the TCS collimators are retracted.

[15] This comes from 1.4.

† The power depostion is similar in the vertical and in the horizontal beam loss scenarios.

† Whatever the energy or plane (hori/vert), the accident scenario is worse (5-30 %) that the nominal one, as expected.

† The worse scenario happens with horizontal losses at top energy and accident conditions. The highest peak power density then reaches 206 $\frac{W}{cm^3}$ (in the third passive absorber), the total power being 49 KW.

The peak power maps in the most heated absorbers are displayed in fig.6.2

Beam loss			hori.			vert.	
Case		TCLPA	TCLSA	TCLQA	TCLPA	TCLSA	TCLQA
nom	inj	2.3 *1.8*	0.15 *0.05*	0.61 *0.35*	2.5 *2.0*	0.1 *0.04*	0.85 *0.56*
	lwb	90 *22.4*	19 *2.7*	212 *39.3*	92 *19.9*	24 *2.8*	188 *36.5*
acc	inj	2.9 *2.3*	0.20 *0.06*	0.67 *0.54*	2.8 *2.0*	0.15 *0.05*	0.67 *0.57*
	lwb	119 *29.3*	34 *3.8*	194 *48.7*	100 *22.0*	27 *3.0*	174 *48.1*

Table 6: Power peaks $[\frac{W}{cm^3}]$ (*and total power* $[kW]$) in the passive absorbers for nominal and accident cases at injection (**inj** = 450 GeV) and top energies (**lwb** = 7000 GeV) in the horizontal and vertical loss scenario of $2 \cdot 10^{16}$ $\frac{protons}{y \cdot beam}$ (Gy/y) and of $4 \cdot 10^{11}$ $\frac{protons}{s \cdot beam}$ (W/cm^3).

7 Collimators

7.1 Heat in the jaws

The collimators filter the primary and secondary halo and therefore they receive a major share of the lost beam energy. Unlike superconducting magnets, heat deposition is not limited by queching phenomena and, consequently, high temperatures are tolerated. However, collimators are delicate components in the sense that they must ensure a precise interacting length and an exact opening between the jaws that filter the halo. If excessive and uneven amounts of heat are deposited in the jaws, deformations may take place and the accuracy of operation can be lost. In the present scenario (*phase I*) heat loads should not entail substantial changes, but for future tasks (*phase II*) solutions are been sought in order to cope with high loss rates while keeping the jaws integrity (rotatable collimators . . .).

The collimators are classified as primary (TC**P**) and secondary (TC**S**), the only difference being the active length of the jaws: 60 cm and 100 cm, respectively. The

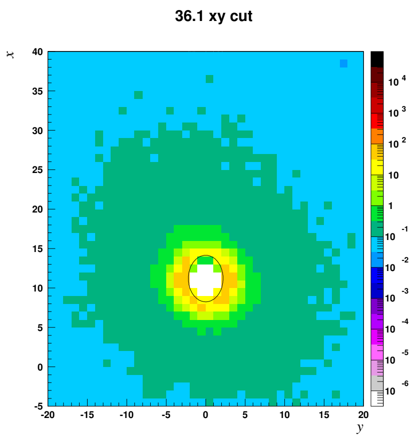

(a) TCLP, cut around z=-47

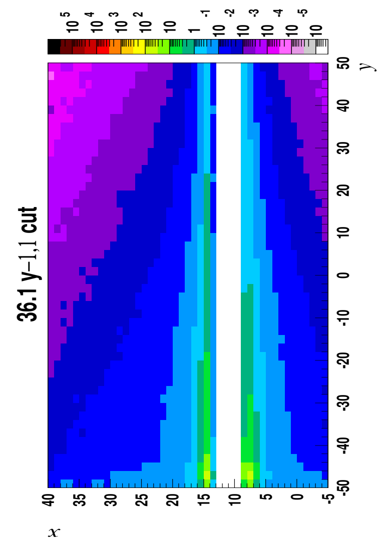

(b) TCLP, cut around y=0

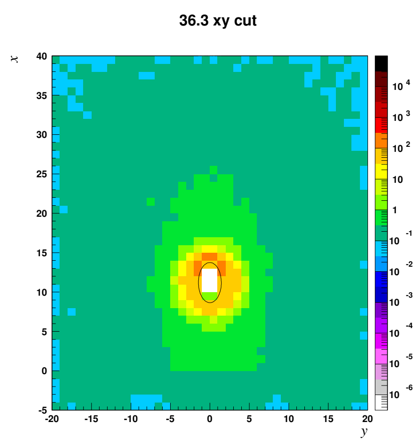

(c) TCLQ, cut around z=-27

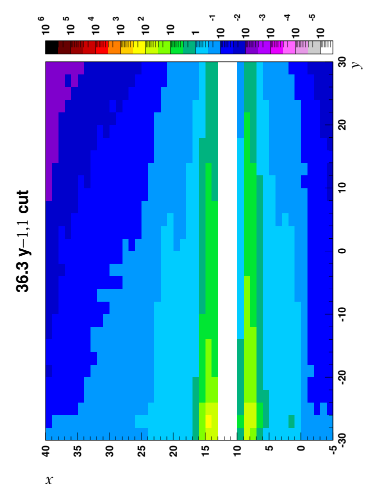

(d) TCLQ, cut around y=0

Figure 6: Peak power deposition $[\frac{W}{cm^3}]$ maps for the 1^{st} and 3^{rd} passive absorbers, for 0.2h beam lifetime at top energy. Note that the scales vary with the secition cut.

underlying idea is to absorb the halo progressively so that the heat is shared among several objects. During the first part of the studies, the TCP's were modelled as 40 cm long objects with 20 cm jaws[16]. Simulations under such conditions reserved the major issues for the TCS's. Later on, it was decided to lengthen the active layer in the jaws of the TCP up to 60 cm[17]. With these assets new loss maps were computed with *Colltrack*[9] and the beam interation files were read by FLUKA for the source of protons. Simulations were carried out for *horizontal* and *vertical* loss scenarios independently.

The heat distribution map (see fig.7.1) in the collimators was computed with FLUKA and the data was exported to ANSYS for temperature distribution mapping and deformation studies (fig.7.1).

The material of the jaws is *carbon*. The heat deposition rate for the horizontal / vertical beam loss scenario with 60 cm long primary active jaws was (full collimator):

† TCPD6: 0.35 W / 2164 W

† TCPC6: 4763 W (676 W in the right jaw) / 12900 W (1650 W in the right jaw)

† TCPB6: 20596 W (2645 W in the right jaw) / 18600 W (3195 W in the *left* jaw)

† TCSGA6: 19085 W (2785 W in the right jaw) / 18325 W (2673 W in the right jaw)

In the frame of *phase II* basic considerations a simulation was run for the hypotetic case of secondary collimators with copper jaws for the horizontal loss scenario at top energy and ultimate intensity. In that case:

† The heat load in TCSGA6L7B1 collimator with copper jaws would reach 110 kW, with 44 kW in each jaw.

7.2 Heat in the coupling fingers

The 80 fingers at each end-cap of the collimators are distributed around the beam forming a collar of inner radius 5.0 cm and outer radius 5.1 cm.

† The total heat deposited in the back fingers of TCSG.A6L7.B1 was 59 W for the whole collar.

[16]While in reality, the *active length* was 20 cm but the jaws were 60 cm long and the rest of the TCP was identical to the TCS.

[17]The rest of the TCP was then identical to the TCS, thus 100 cm long.

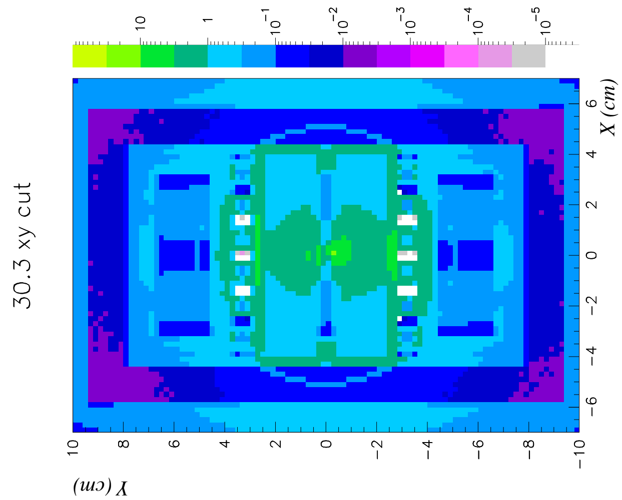

(a) Heat deposition in TCPB6L1

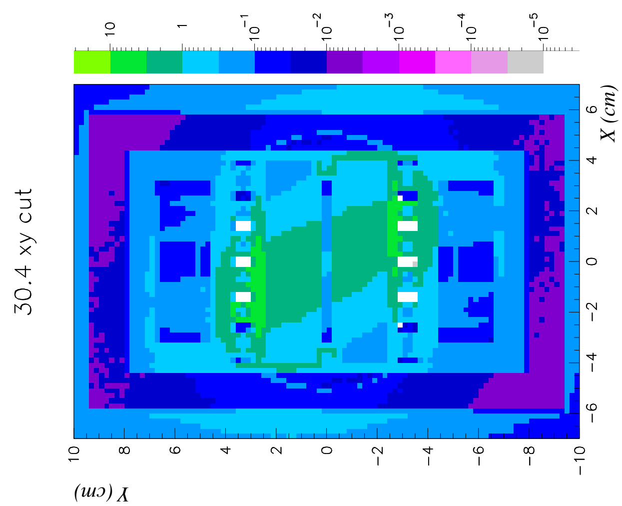

(b) Heat deposition in TCSGA6L1

Figure 7: Cross sectional energy deposition plots $[\frac{W}{cm^3}]$ in the hotest collimators for the horizontal beam loss scenario.

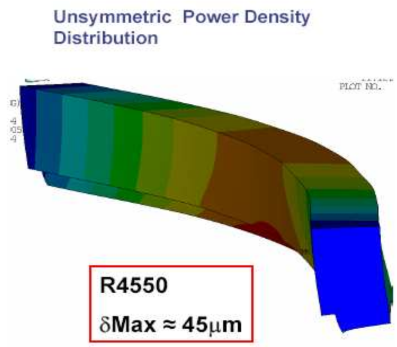

Figure 8: Deformation studies of the jaws[10]

† The angular heat distribution in the fingers is tabulated in 7.3. These apparently don't compromise the operation of the collimators.

7.3 Assymetric irradiation of the flanges

Fig.7.3 shows the estimated heat distribution in the flanges of TCSG.A6L7.B1 for different transverse directions.

Element	**45°**	**90°**	**135°**	**180°**	**TOT** $[W]$
Fingers	1.7	1.8	2.3	2.2	59
Inner Flange	1.6	1.9	2.5	1.9	325

Table 7: Heat distributions $[\frac{W}{cm^3}]$ in sensitive elements of the TCSG.A6L7.B1 (downstream components).

† The total heat and the anisotropy remain tolerable.

A Singularities of FLUKA implementation of the straight section

A.1 Settings

Simulations were carried out for the straight section in order to obtain the energy deposition rates in the warm elements. The present file system allows defininining customized set-ups for different environments. As for the straight section, the user must trigger the following options in the input file (ir7.fluka):

- comment the card: *#define EMFCUT* → ⋆*# define EMFCUT*
- **un**comment the card: ⋆*# define LOWIMPRR* → *#define LOWIMPRR*
- **un**comment the card: ⋆*# define SCRCOL* → *#define SCRCOL*
- comment the card: *#define SCRCOLD* → ⋆*# define SCRCOLD*

The "define EMFCUT" sets the EMF threshold to 100 MeV for electrons and 10 MeV for photons in the straight section. It should only be used to speed the simulations by reducing the accuracy of energy deposition in the straight section. The define LOWIMPRR reduces the region importance (via BIASING) in the RR and UJ cavities. It should be commented for simulations dedicated to the cavities. SCRCOL turns on/ooff the power deposition scorings in the collimators. The define SCRCOLD activates the scoring cards relative to the curved section.

A.2 Geometry description

Passive absorbers were included in the IR7 geometry by means of **LATTICE**. As for the other elements, the user should implement the prototype in the parking and specify the position in the tunnel of the replica. From this information, the script **mklattic.r** generates the necessary **lattic.f** file. This section presents the steps the user should follow to modify the shape and position of the passive absorber and to setup 'dose' detectors.

The passive absorber is a block of steel, defined as an RPP body. The alternatives are to use one (and only one) of the pre-defined RPP bodies (PA_BODY or PAsBODY), to modify one of them or to create a new one. The only constraints are that the RPP should fit in the available parking area and that there is no overlapping with other existing body (e.g., PA_BODY, unless commented). The hole for the beam (representing the beam chamber) is defined near the RPP.

In the IR7 directory there is a file, **prototype.pos** containing the element name (e.g. TCLP, TCLS, TCLQ are prototypes of several passive absorbers), two parameter (integer numbers), the RPP name, the centre of rotation (simply the centre of the RPP for the TCLP) and the length of the prototype. The last column could be filled with the symbol '-', to indicate that no magnetic field is defined. The two parameters should be assigned the value of 1 (the box should be subtracted from both beams, which is true for wide absorbers) and 1 (if there are two passive absorbers with the same name but one for beam 1 and the second for beam 2, they are treated as the same object and therefore implemented only once). Please note that the file prototype.pos is not copied in the running directory and applies to all following simulations. If a major change is done, it is wise to copy the file to the running directory for future use. If no passive absorber is needed, the presence of a line in this file indicating the name of the absorber RPP is of no consequence.

In the IR7/Twiss directory there are two important files: absorber_summary.dat and **V6.5_absorbers.b1.phase1.data**. The former contains information on the active absorbers and should not be touched in this case. The latter describes the position of the absorber (fifth column). The position is given in meters, *absolute coordinates*, Z, and refers to the starting (min z) of the object (not the center)[18]. If no passive absorber is needed, the line with the position of the passive absorber should be deleted. If more absorbers are needed, new lines can be added.

In brief, these are the steps to introduce a passive absorber:

1. Define the RPP and ZEC bodies for the box and pipe hole in ir7.fluka (eg. PA_BODY, PA_hole).
2. Define the region of the PA (e.g. `PA_YOKE 25 +PA_BODY -PA_HOL1`).
3. Remove PA_YOKE from the rest of the tunnel (PARK_AIR).
4. Assign a material to the PA_YOKE (e.g. `ASSIGNMAT TUNGSTEN PA_YOKE`).
5. Register the body of the PA in prototype.pos (e.g. `TCLP 1 1 PA_BODY -2000.0 0.0 -750.0 100.0 -`)
6. Add the PA (here it would be TCLP...) description in V6.5_absorbers.b1.phase1.data (absolute coordinates).

A.3 Technical information about scoring in the MBW and MQW

In order to score the energy deposition in the MBW and MQW, USRBIN cards were defined. The output units are 31 for MBW, 35 for MQW, 34 for the pipes

[18] $Z = 199.9416 + 0.01 \cdot z$

in MBWB and MQWAE and 36 for the PA. To what it concerns the MBW, there are two families of USRBIN: one for the dipole as a whole and one for the coils that come out of the main box, which are the most exposed to radiation. As for all the other elements, the boundary limits of the USRBIN geometry are given in the reference system of the element starting from the element center. Energy scorings produce results in GeV/cm^3. To obtain doses, one should normalize these values by the material density[19] which is function of the region. To obtain doses, it is therefore better to use cards with a SDUM beginning with 'D:', in which case a special routine is called to do the region(material)-dependent normalization. Note that the "D:" prefix can only be inserted in the preprocessed ".inp" input file but not directly in the ".fluka" file[20].

The density of the insulator should be used for values referring to the region

[19] As shown in eq. 1.

[20]

- **usrbin_36**: A 1 x 1 x 2 cm^3 $\{x, y, z\}$ mesh grid scoring per passive absorber (3).
- **usrbin_31**: 12 cartesian binned scorings referred to the MBW's:
  1. Power in full **MBWB**. 1 x 1 x 5 cm^3
  2. Power in full **MBWA**. 1 x 1 x 5 cm^3
  3. Power in upfront coil of **MBWB**. 1 x 1 x 1 cm^3
  4. Power in lowfront coil of **MBWB**. 1 x 1 x 1 cm^3
  5. Power in upback coil of **MBWB**. 1 x 1 x 1 cm^3
  6. Power in lowback coil of **MBWB**. 1 x 1 x 1 cm^3
  7. Power in upfront coil of **MBWA**. 1 x 1 x 1 cm^3
  8. Power in lowfront coil of **MBWA**. 1 x 1 x 1 cm^3
  9. Power in upback coil of **MBWA**. 1 x 1 x 1 cm^3
  10. Power in lowback coil of **MBWA**. 1 x 1 x 1 cm^3
  11. Dose in entire **MBWB**. 1 x 1 x 5 cm^3
  12. Dose in entire **MBWA**. 1 x 1 x 5 cm^3
- **usrbin_34**: 2 Dose deposition scorings in cartesian meshs in MBWB and the MQWAE:
  1. 1^{st} (z) half of the elliptical pipe of **MBWB** 0.1 x 0.1 x 2 cm^3
  2. 1^{st} (z) half of the elliptical pipe of **MQWAE** 0.1 x 0.1 x 2 cm^3
- **usrbin_35**: 6 annual dose scorings in cartesian meshs within MQWAEL7 and MQWADL7:
  1. first 2 cm of **MQWAEL7** 1.0 x 1.0 x **2.0** cm^3
  2. next 2 cm of **MQWAEL7** 1.0 x 1.0 x **2.0** cm^3
  3. rest of **MQWAEL7** 1.0 x 1.0 x **3.1** cm^3
  4. first 2 cm of **MQWADL7** 1.0 x 1.0 x **2.0** cm^3
  5. next 2 cm of **MQBWADL7** 1.0 x 1.0 x **2.0** cm^3
  6. rest of **MQWADL7** 1.0 x 1.0 x **3.1** cm^3

between the coils, whereas the density of the coil should be used for the coils themselves, which were assigned copper as material. The annual dose in the epoxy present in the coils should be calculated by using the proper coefficient of the coils.

B Data for the passive absorbers simulations

B.1 Data analysis scripts

When running the code, the results for the USRBIN are stored in the binary files *⋆.fort_num⋆*, where *num* is to be replaced by 31, 34 , 35 or 36 (see A), and 39. The program *usbsuw* collects the results from different runs and computes the mean and variance, *ustfuf* transform the binary results to ASCI and *EnLattice.pl* takes the formated and averaged results 39 (energy in every object) and the input file description (ir7.inp) to produce the *LatticeWatt* table of results with the energy deposition in every single component of all objects.[21]

B.1.1 The *anStraight.sh* script

All these scripts are confortably managed by *anStraight.sh*, which takes care to add results of new runs to the preexisting summary files.

```
#!/bin/bash
#usrdo.r ./*/*out ./*/*_fort.*
#set -x
echo "Analysis & Graphs (1), Analysis only (2), Graphs Only (3)?"
read answer1
if [ $answer1 -ne 3 ] # want analysis
then
ls usrbin_39
if [ $? -eq 0 ]
then
  echo "Redo Analysis (R), Add data (A), or only do Graphs (G)? (R/A/G)"
  echo " add data means that new fort files are added to usrbin_"
  echo " remember then to delete the old fort files !!"
else
  echo "Redo Analysis (R), or only do Graphs (G)? (R/G)"
fi
read answer
if [ $answer = R ]
then
input=`ls ./*/*.out | head -n1`
min=1
max=250
#i=fort file ...
bash usrdon.sh $min $max #$i
$IR7/Processing/usbfuf <<EOF
```

[21]The third input parameter for *EnLattice.pl* is whether there is one or two beams acting (needed to normalize). Normally only one beam is considered at the time.

```
y
usrbin_39
usrbinf_39
EOF
input=`ls ./*/ir7.inp ir7.inp | head -n1`
echo "******* input= $input"
perl EnLattice.pl <<EOF
${input}
usrbinf_39
1
EOF
elif [ $answer = A ]
then
ls ./[0-9]*/*fort.* | sed s/fort./#/ | cut -d# -f2 | sed /^77$/d
 | sort | uniq > listfort
nfort=`cat listfort | wc -l`
i=1
while [ $i -le $nfort ]
do
   fort=`cat listfort | head -n$i | tail -n1`
   n=`ls -ltr ./*/*fort.$fort usrbin_$fort | cut -d: -f2 | sed 's/ /#/'
 | cut -d# -f2 | grep -n usrbin | cut -d: -f1`
   nl=`ls -ltr ./*/*fort.$fort usrbin_$fort | cut -d: -f2 | sed 's/ /#/'
 | cut -d# -f2 | wc -l`
   nf=`expr $nl - $n + 1`
   ls -ltr ./*/*fort.$fort usrbin_$fort | cut -d: -f2 | sed 's/ /#/'
 | cut -d# -f2 | tail -n$nf >listev
   echo " ">>listev
   echo "usrbin_${fort}">>listev
   echo "here is the list for fort $fort:"
   cat listev
   cp usrbin_$fort usrbin_$fort.bck
   $IR7/Processing/usbsuw<listev
   cp usrbinf_$fort usrbinf_$fort.bck
$IR7/Processing/usbfuf<<EOF
y
usrbin_$fort
usrbinf_$fort
EOF
    i=`expr $i + 1`
done
input=`ls ./*/ir7.inp | head -n1`
echo "******* input= $input"
perl EnLattice.pl <<EOF
${input}
usrbinf_39
1
EOF
fi
fi  # analysis vs. graphs
if [ $answer1 -ne 2 ]  ##---> want graphs
then
   ns=`find ./* -name *fort.29 | grep -cv fluka*`
   echo "ns=$ns"
   echo $ns >results
   # fingers:
```

```
  bash plotrphi.sh 27 2
  # flanges:
  bash plotrphi.sh 29 8
  # collimator jaws
  bash plotxyxz.sh 30 4 #(only beam1)#
  ls graphs
if [ $? -ne 0 ]
then
  mkdir graphs
fi
## Energy in elements per unit length:
  usbmax -d 2 -o elmeter.dat usrbin_39
  echo "1">input
  echo "set gfont -30">>input
  echo "set gsiz 0.4">>input
  echo '*opt grid'>>input
  echo 'opt logy'>>input
  echo "title 'Density of energy in elements/length '">>input
  echo "f/file 60 elmeter.ps">>input
  echo "meta 60 -111">>input
  echo "null -6000 36000 0 1">>input
  echo "set gfont -30">>input
  echo "set gsiz 0.4">>input
  echo "set asiz 0.35">>input
  echo "set lwid 4.3">>input
  echo "set plci 2">>input
  echo "opt logy">>input
  echo "v/read x,y,z,r1,r2,r3,r4,max,err elmeter.dat ! ! -/#/">>input
  echo 'graph $vdim(z) z $sigma(max*57600) l'>>input
  echo "atitle 'z (cm)' 'E?max!/V (mW/cm^3!)' ! 222">>input
  echo 'g/h/error z $sigma(max*57600) $sigma(z*0) $sigma(max*57600*err*0.01)
 $vdim(z) 2 1 l'>>input
  echo "for/close 60">>input
  echo "quit">>input
  paw<input
# Energy in the tunnel
  usbmax -d 5 -o tunnel.dat usrbin_39
  echo "1">input
  echo "set gfont -30">>input
  echo "set gsiz 0.4">>input
  echo '*opt grid'>>input
  echo 'opt logy'>>input
  echo "title 'Density of energy in tunnel.A6.R7'">>input
  echo "f/file 60 tunnel.ps">>input
  echo "meta 60 -111">>input
  echo "null -6000 30000 0 1000">>input
  echo "set gfont -30">>input
  echo "set gsiz 0.4">>input
  echo "set asiz 0.35">>input
  echo "set lwid 4.3">>input
  echo "set plci 2">>input
  echo "opt logy">>input
  echo "v/read x,y,z,r1,r2,r3,r4,max,err tunnel.dat ! ! -/#/">>input
  echo 'graph $vdim(z) z $sigma(MAX*57600) l'>>input
  echo "atitle 'z (cm)' 'E?max!/V (mW/cm^3!)' ! 222">>input
  echo 'g/h/error z $sigma(MAX*57600) $sigma(z*0) $sigma(MAX*57600*ERR*0.01)
```

```
 $vdim(Z) 2 1 1'>>input
  echo "for/close␣60">>input
  echo "quit">>input
  paw<input
  mv *.ps graphs
fi  # graphs analysis
```

B.1.2 The *plotrphi.sh*, *plotxyxz.sh*, *plotMBW.sh* and *plotMQW.sh* scripts

In order to visualize the energy deposition/dose maps the general purpose programs *plotrphi.sh*, *plotxyxz.sh* or the particulized *plotMBW.sh*, *plotMQW.sh* (all based in pawlevbin) can be used, the latter ones superimposing the geometry over the color plots.

```
#!/bin/bash
if [ $# -eq 2 ]
then
# use coilan.sh usrbin# bin#. for coils usrbin_33, bin 1
i=1
while [ $i -le $2 ]
do
   #phi-cut
   echo "␣">input1    # no plotgeom
   echo "␣">>input1
   echo "usrbin_$1">>input1
   echo "-0.0173611">>input1 # 4E11 * 0.9 * 1.6E-10 w/cm3
   echo "␣">>input1
   echo "$i">>input1 # select bin
   echo "␣">>input1  # Rmin Rmax
   echo "␣">>input1  # R  phy-z cut
   echo "␣">>input1  # Phimin Phimax
   echo "␣">>input1  # Phi  R-z cut
   echo "␣">>input1  # zmin zmax
   echo "1">>input1  # nz  xy cut
   echo "␣">>input1
   echo "␣">>input1
   pawlevbin<input1
   #
   # Now I plot the pawlev files with paw, z cut
   #
   echo "␣">input1
   echo "exe␣$FLUPRO/flutil/pawlevphi">>input1
   #echo "␣">>input1
   echo "$1.$i.ps">>input1   # output file
   echo "bin␣$i,␣z␣cut">>input1   # title
   echo "␣">>input1  #pawlev
   echo "␣">>input1  #x min
   echo "␣">>input1  #x max
   echo "␣">>input1  #y min
   echo "␣">>input1  #y max
   echo "N">>input1  # geometry only
   echo "1E-2">>input1   # minval  1E-4
   #echo "1E-2␣">>input1   # maxval 1E3
```

```
    echo "4">>input1   # divisions per decade 57
    paw<input1
    i=`expr $i + 1`
done
else
echo "need␣usrbin␣and␣max␣number␣of␣bins␣to␣analyze" 58
fi
```

B.1.3 Parsing the peak value with zone exceptions: *getstat*

A visual inspection of the dose/energy deposition plots for different sections of MBW and MQW gives a good idea of the peak values reached in the coils. However, if precise numbers are needed, then the result files must be inspected to parse the peak value, taking the precaution to discard the numbers that don't belong to the coils[59] or to whatever sensitive component we want to protect.

The program *getstat* (available at *[scripts]*) solves the peak identification inside bounded regions. To run it do the following:

1. Create a mask to discard/accept bins according to the region number: This can be done by editing *comscw.f* (see B.2) and making a short dummy run with the source shining directly on the magnet whose output will contain zeros in the irradiated regions that are not made of copper..

2. Use *anStraight.sh* (see B.1.1) to produce the formatted file, eg. usrbinf_35.coil

3. Run the normal simulation with the 'D:...' card in the SDUM of the concerned usrbin to force *dose* calculation (again consult B.2).

4. Use *anStraight.sh* (see B.1.1) to produce the formatted file, eg. usrbinf_35

5. Run getstat

   a) **Q:** input file name? e.g: usrbinf_30 **A:** usrbinf_35
   b) **Q:** scaling factor? e.g: 2238 (GeV/cm3 p → MGy/y) **A:** 2E3 [60]
   c) **Q:** minimum corner: Xmin Ymin Zmin [cm]? **A:** -300 -300 -300[61]
   d) **Q:** maximum corner: Xmax Ymax Zmax [cm]? **A:** +300 +300 +300

6. The results are printed in the screen.

[59] Typically they are quite complex, so no mesh (cartesian or cylindrical) will match the coil shape.

[60] To obtain MGy/y in the MQW coils (results are directly normalized to density through comscw.f) for a loss irradiation of $2 \cdot 10^{16}\ \frac{protons}{beam \cdot y}$. Alternatively use 444 for the MBW coils, to account for the density factor, not included in the calculations (see the introduction, 1.4).

[61] This is used to restrict the search to a box. Put big numbers to include everything.

B.2 User defined subroutines: *comscw.f*

The subroutine *[src]/comscw.f* can be edited to score only in region selected areas within a given usrbin. In the example shown in B.2 events are only scored if the current cell (Mreg) is among the provided list (in the **IF ... THEN** check).

```
...
      IF (ISCRNG.EQ.1) THEN
         IF (TITUSB(JSCRNG)(1:2) .EQ. 'R:') THEN
* For insulators in MQW PAlimitWsW
            IF (Mreg.eq.209.or.Mreg.eq.210.or.Mreg.eq.211.or.Mreg.eq.212
     $            .or.Mreg.eq.218.or.Mreg.eq.219.or.Mreg.eq.225.or.Mreg
     $            .eq.226.or.Mreg.eq.232.or.Mreg.eq.233.or.Mreg.eq.239.or
     $            .Mreg.eq.240.or.Mreg.eq.246.or.Mreg.eq.247.or.Mreg.eq
     $            .253.or.Mreg.eq.254.or.Mreg.eq.260.or.Mreg.eq.261) THEN
            IF (Mreg.eq.209.or.Mreg.eq.210.or.Mreg.eq.212.or.Mreg.eq.216
     $            .or.Mreg.eq.217.or.Mreg.eq.219.or.Mreg.eq.223.or.Mreg
     $            .eq.224.or.Mreg.eq.226.or.Mreg.eq.230.or.Mreg.eq.231.or
     $            .Mreg.eq.233.or.Mreg.eq.237.or.Mreg.eq.238.or.Mreg.eq
     $            .240.or.Mreg.eq.244.or.Mreg.eq.245.or.Mreg.eq.247.or
     $            .Mreg.eq.251.or.Mreg.eq.252.or.Mreg.eq.254.or.Mreg.eq
     $            .258.or.Mreg.eq.259.or.Mreg.eq.261) THEN
              COMSCW = 1
            ELSE
              COMSCW = 0
            END IF
* For coils in MQW
            IF (Mreg.eq.221.or.Mreg.eq.222.or.Mreg.eq.228.or.Mreg.eq.229)
     $            THEN
              COMSCW = 1
            ELSE
              COMSCW = 0
            END IF
         ENDIF
         IF (TITUSB(JSCRNG)(1:2) .EQ. 'D:') THEN
            COMSCW = ELCMKS*1.D12 / RHO (MEDIUM(MREG))
         ENDIF
      ENDIF
     $
...
```

The annual dose can be computed “on-line” checking bin by bin the density of the hosting material. This is the most correct and practical way for dose computations, specially for big gradients of density.

```
         IF (TITUSB(JSCRNG)(1:2) .EQ. 'D:') THEN
            COMSCW = ELCMKS*1.D12 / RHO (MEDIUM(MREG))
         END IF
```

References

[1] A. Fassò, A. Ferrari, S. Roesler, P.R. Sala, G. Battistoni, F. Cerutti, E. Gadioli, M.V. Garzelli, F. Ballarini, A. Ottolenghi, A. Empl, and J. Ranft. The physics models of FLUKA: Status and recent developments. In *Computing in High Energy and Nuclear Physics 2003 Conference (CHEP2003), La Jolla, CA, USA, March 24-28, 2003*, volume arXiv:hep-ph/0306267, March 2003.

[2] A. Fassò, A. Ferrari, J. Ranft, and P.R. Sala. *FLUKA: a multi-particle transport code*. CERN, INFN, SLAC, 2005.

[3] R. Assmann and A. Ferrari. Addition of absorbers to IR7 and IR3. Engineering Change Request - Class I 692481, CERN, February 2006.

[4] M. Magistris, M. Santana-Leitner, V. Vlachoudis, and A. Ferrari. Optimization of the active absorber scheme for the protection of the dispersor supressor. Technical report, CERN-AB-ATB, 2006.

[5] M. Santana-Leitner, V. Vlachoudis, A. Ferrari, M. Magistris, and K. Tsoulou. Energy deposition studies for the betatron cleaning insertion. In Particle Accelerator Conference 05, editor, *PAC05 proceedings*, CERN CH-1211 Geneva-23 Switzerland, 2005. CERN-AB.

[6] S. Ramberger. Review of radiation limits of the IR3/IR7 warm magnets. http://lhc-collimation.web.cern.ch/lhc-collimation/library_talks.htm.

[7] Lamont M. Estimates of annual proton doses in the lhc. Lhc project note, CERN AB/OP, October 2005. 375.

[8] R. Assmann and A. Ferrari. Passive absorbers and increase of inter-distance between d3 modules in IR7. Engineering change request - class i, CERN, February 2006.

[9] G. Robert-Demolaize, R. Assmann, S. Redaelli, and F. Schmidt. A new version of sixtrack with collimation and aperture interface. In Particle Accelerator Conference 05, editor, *PAC05 proceedings*, CERN CH-1211 Geneva-23 Switzerland, 2005. CERN. Published.

[10] A. Bertarelli et al. Mechanical design for robustness of the LHC collimators. In Particle Accelerator Conference 05, editor, *PAC05 proceedings*, CERN CH-1211 Geneva-23 Switzerland, 2005. CERN. Published.